Top illuminated inverted organic ultraviolet photosensors with single layer graphene electrodes

Martin Burkhardt, Wei Liu, Christopher G. Shuttle, Kaustav Banerjee, and Michael L. Chabinyc

Citation: Appl. Phys. Lett. **101**, 033302 (2012); doi: 10.1063/1.4733299

View online: http://dx.doi.org/10.1063/1.4733299

View Table of Contents: http://apl.aip.org/resource/1/APPLAB/v101/i3

Published by the American Institute of Physics.

Top illuminated inverted organic ultraviolet photosensors with single layer graphene electrodes

Martin Burkhardt,[1] Wei Liu,[2] Christopher G. Shuttle,[1] Kaustav Banerjee,[2,a)] and Michael L. Chabinyc[1,b)]
[1]*Materials Department, University of California Santa Barbara, California 93106-5050, USA*
[2]*Department of Electrical and Computer Engineering, University of California Santa Barbara, California 93106, USA*

(Received 22 April 2012; accepted 19 June 2012; published online 16 July 2012)

Inverted, top-illuminated organic photodiodes are demonstrated using transparent electrodes including single layer graphene (SLG) and thin gold or silver with poly(3-hexylthiophene) and 1 -(3-methoxycarboyl)-propyl-1-phenyl-(6,6)C_{61} as active layer. The devices are free of both indium-tin-oxide and poly(3,4-ethylenedioxythiophene):poly(styrene-sulfonate). The maximum solar power conversion efficiencies were 0.3% for SLG due to its series resistance and ~2% for gold and silver. The organic photodiodes with SLG electrodes had good external quantum efficiency at incident illumination less than 10 mW/cm^2 and better performance than gold and silver at wavelengths below 300 nm making them attractive for ultraviolet photosensors. © *2012 American Institute of Physics*. [http://dx.doi.org/10.1063/1.4733299]

Inorganic photodetectors using GaN, SiC, Si, and GaAs cover three important spectral sub-bands of light, the ultraviolet (UV), visible, and near infrared (NIR).[1] Recently, organic photodiodes comprising electron donating and electron accepting materials have been demonstrated to have broad spectral responses (350–1450 nm) with photodetectivities exceeding 10^{12} Jones.[2,3] The response at both short (UV) and long (near-IR) wavelengths in the same device is a particularly interesting feature of organic photodetectors. High detectivity in the UV region is important for future generation, high energy radiation sensors that use scintillation layers.[4] In addition to the wide spectral response, organic materials enable large area processing on inexpensive substrates (glass or polymeric foils) and can be used in low-cost applications such as large area solar cells.[5]

The device structures of organic photodetectors and solar cells can have an important impact on their performance. Both are typically made in a structure where the light shines through a transparent electrode, such as indium tin oxide (ITO), on a transparent substrate.[6] In "conventional" cells, ITO acts as the anode and collects the photogenerated holes while for electron collection the other electrode (cathode) is chosen to have a lower work function, e.g., Al. In "inverted" devices, the ITO electrode is typically coated with a wide band gap metal oxide with a conduction level that is aligned to the unoccupied electronic level of the acceptor in the organic layer to collect electrons while the other electrode (anode) is chosen to have a higher work function, e.g., Ag to collect holes.[6] However, in both cases, the photodiodes are illuminated through the substrate. In contrast, illumination from the top electrode, whether it is the anode or cathode, is desirable to allow the use of non-transparent substrates and also to aid in integration with electronics such as imaging arrays[7] where the underlying electronics may reduce the illuminated area of the photosensor or be opaque, e.g., a silicon IC or polysilicon on stainless steel.[8] Currently, it is difficult to deposit the most commonly used transparent electrode, ITO, onto organic materials due to damage to the organic layer during the deposition process.[9] Alternative transparent electrodes including poly(3,4-ethylenedioxy-thiophene):poly(styrenesulfonate) (PEDOT:PSS),[5,10] silver nanowires,[11] and thin metal layers (gold)[12] have been demonstrated, but their performance as transparent electrodes with top illumination have not been widely studied.

We report here the performance of inverted bulk heterojunction (BHJ) organic photosensors of poly(3-hexylthiophene) (P3HT) and [6,6]-phenyl-C_{61}-butyric acid methyl ester (PCBM) with transparent top electrodes that exhibit efficient detection of light from the UV to the visible region (~250 nm to 650 nm) (Figs. 1 and 2). A critical need for broad spectral response with top illumination is a transparent electrode with optical transmission higher than 85% over the desired spectral range. In this work, we investigated (semi)-transparent top anodes using conventional metals including Ag and Au (approx. 50% transmittance), and also single layer graphene (SLG, 85% transmittance, see supplementary data[34]). SLG films have recently been grown over large areas using chemical vapor deposition on metallic foils[13,14] eliminating the difficulty of forming large-area exfoliated films

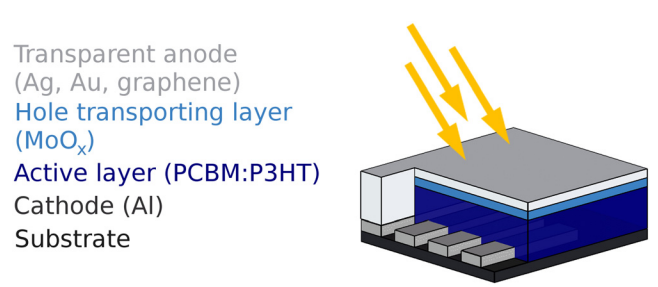

FIG. 1. Schematic view of an inverted photosensor (not to scale) with top illumination; substrate (black), P3HT:PCBM (1:0.8) active layer (blue), MoO_x (light blue), and anode (white).

a)Electronic mail: kaustav@ece.ucsb.edu.
b)Electronic mail: mchabinyc@engineering.ucsb.edu.

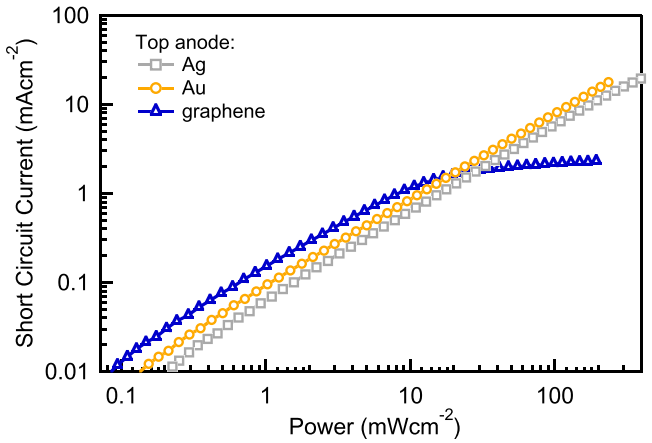

FIG. 2. Short circuit current as a function of monochromatic red light intensity (red LED illumination, wavelength ~625 nm) of top-illuminated inverted photosensors with (semi-)transparent top anodes (Ag, Au, SLG).

for electrodes.[15] SLG is particularly attractive because it has high transparency over a broad spectral range, high mechanical flexibility,[16,17] and can act as a gas barrier for encapsulation of the underlying organic layer.[18] Most prior studies of BHJ photodiodes with graphene electrodes have focused on either the conventional[19–21] or inverted geometry[22] with illumination through the substrate in contrast to the top-illuminated devices examined here. All of the photodiodes examined here are free of both ITO and also PEDOT:PSS, which is known to have significant thermal and chemical instabilities.[23,24]

All devices were prepared on solvent cleaned glass substrates on which the patterned aluminum cathode (thickness of 50 nm) was evaporated. The P3HT:PCBM solution was spin coated (weight ratio: 1:0.8) to obtain layer thicknesses of 210–230 nm, followed by annealing in the presence of ortho-dichlorobenzene, and thermal annealing at 150 °C (10 min).[25] For some devices, molybdenum(VI)oxide (~10 nm at 0.2 Å/s, 99.99%, Sigma Aldrich) was evaporated as a hole transporting layer prior to processing of the (semi)-transparent Ag and Au anodes (10 nm). High quality SLG was grown on copper using optimized low pressure chemical vapor deposition yielding films with large grain size (100–200 μm) and carrier mobilities exceeding 3500 cm^2/Vs.[26] To mechanically stabilize large-scale continuous SLG, a thin layer of poly(methyl methacrylate) (PMMA, MicroChem950 C2) was spin-coated on top of SLG/copper. The PMMA/SLG/Cu films were baked at 180 °C for 10 min prior to etching the copper by iron nitrate. The PMMA/SLG films were cleaned with dilute HCl and DI water and then transferred to the photodetector device and annealed for 5 min at 120 °C. The finished devices were characterized as solar cells using an AM 1.5 solar simulator under 100 mW/cm^2 top illumination (Table I). Their spectrally resolved external quantum efficiency (EQE) was measured using monochromatic light source comprising a 300 W Xe lamp and a monochromator (Newport Cornerstone 260). The incident intensity was 5 mW cm^{-2} or less and the photocurrent was amplified by a current preamplifier (SRS SR570) and recorded by a lock-in amplifier (SRS SR810). A calibrated Si photodiode (Newport 818-UV) was used as a reference. DC bias was applied to the device by a source-measure unit (Keithey 2602 A).

The top-illuminated, inverted devices with metal electrodes had the highest efficiency as solar cells. The power conversion efficiencies (PCE) of devices with Ag and Au electrodes were best with an additional layer of MoO_x, a wide-gap oxide whose conduction level is aligned to the HOMO of P3HT, and are given in Table I. The open circuit voltage (V_{OC}) and series resistance (R_S) were both dependent on the presence of the MoO_x layer. Without MoO_x, the V_{OC} was 0.43 V for Au and was 0.29 V for Ag, however, they were nearly identical (~0.58 V) with the MoO_x layer. We attribute the difference to a change in the line-up of the HOMO of P3HT with the electrode due to *p*-type doping of P3HT by MoO_x.[27] This hypothesis is also consistent with the higher series resistance of devices without the MoO_x layer (R_S(Au): 120 Ωcm^{-2}; R_S(Ag): 166.9 Ωcm^{-2}) compared to those with it (R_S(Au): 13 Ωcm^{-2}; R_S(Ag): 28 Ωcm^{-2}).

The characteristics of top-illuminated solar cells with a SLG electrode are substantially worse than those with metal electrodes due to the higher series resistance from the undoped SLG. Inverted cells with SLG and a contact layer of MoO_x give PCE of 0.19% with V_{OC} of 0.55 V, J_{SC} of 1.8 mA/cm^2, FF of 19%, and R_S of 267 Ωcm^{-2}. Despite the low value of the PCE, we believe that it is the highest reported for a top illuminated inverted organic solar cell using a SLG anode. The J_{SC} of devices with Ag and Au top anodes has a linear dependency on light intensity to higher than 2 suns illumination (see Figure 2). In contrast, the J_{SC} of devices with SLG as transparent electrode shows a linear light dependency up to only 10 mW cm^{-2}. Due to the R_S, the J_{SC} is limited for higher light intensities with saturation at approximately 2 $mAcm^{-2}$. Similar low efficiencies have been observed in dye-sensitized[28] and small molecule-based[29] solar cells under 1 Sun conditions with top illumination through SLG. Additionally, large SLG sheets (sheet size: approx. $15 \times 10\,mm^2$) are transferred onto the Al/P3HT:PCBM/MoO_x stack resulting in defects such as physical discontinuities and as a result mechanical stress may affect R_S and J_{SC} in some devices. We expect that the wet transfer process in air may affect the V_{OC} due to changes in the stoichiometry of MoO_x and the J_{sc} and FF through formation of defect states in the BHJ[30] as well. The SLG devices operate efficiently under low light (*vida infra*), therefore we believe that the contribution of the series resistance dominates formation of trap states during fabrication. Nonetheless, these devices are significant because the BHJ layer is exposed to the ambient atmosphere and water during processing and the final devices still exhibit good performance as photodiodes.

Inverted, top-illuminated photodiodes with SLG perform well as photosensors at low incident light intensity and have improved EQE at short wavelengths compared to photodiodes with metal electrodes. The EQEs of devices with SLG, Ag, and Au electrodes were recorded at −0.1 V bias (Figure 3). The reverse bias was chosen to limit irreversible damage of SLG that was observed at biases beyond −0.5 V. The EQE characteristics for all devices correlate well to the transmittance of the (semi-)transparent electrodes and the absorbance of P3HT:PCBM (for detailed UV-Vis spectra, see supplementary data). The EQE is ~30% over a broad range using a SLG top electrode due to its homogeneous high transmittance (>85%). In contrast, semitransparent Au and

TABLE. I. Performance parameters for top illuminated inverted photosensors with variation in the device structure: substrate (glass)/Al/active layer (P3HT:PCBM, 1:0.8)/hole transporting layer (MoO_x)/(semi-)transparent anode (Ag, Au, SLG). The values given include the PCE, short circuit current (J_{SC}), open circuit voltage (V_{OC}), fill factor (FF), shunt resistance (R_{Sh}), and series resistance (R_S). Values for average devices are given with best results in parentheses.

Anode	PCE [%]	J_{SC} [mA/cm^2]	V_{OC} [V]	FF [%]	R_{Sh} [MΩ cm^{-2}]	R_S [Ω cm^{-2}]
Silver	1.4 (2.0)	4.4 (6.1)	0.58 (0.58)	54 (57)	3.4 (1.0)	28 (4.2)
Gold	1.6 (1.9)	4.9 (5.6)	0.59 (0.59)	55 (59)	6.7 (6.0)	13 (3.9)
SLG	0.19 (0.30)	1.8 (2.6)	0.55 (0.58)	19 (19)	2.9 (11.0)	267 (297)

Ag top electrodes result in average values around 20% with maximum signals (35% and 30%) at 300–400 nm for Ag and 480–600 nm for Au. Devices with SLG outperform those with both Ag and Au at wavelengths less than 300 nm.

To evaluate the performance of the top-illuminated organic photodiodes as sensors, we calculated their responsivity and estimated their detectivity, the inverse of the noise equivalent power (Figure 4). The spectral current responsivity (R_λ in A/W) is given as:[31]

$$R_\lambda = \frac{\lambda\eta}{hc} qg, \tag{1}$$

with wavelength (λ), quantum efficiency (η), Planck's constant (h), the electric charge (q), and the photoelectric gain (g). Assuming the extraction of one charge carrier per electron hole pair, the value of gain is 1. The detectivity (D^*_λ) was calculated assuming that the shot noise was the dominant noise source as:[2]

$$D^*_\lambda = R_\lambda / \sqrt{2qJ_{dark}} \tag{2}$$

with the dark current (J_{dark}).[32] In imaging applications, the detectivity could be lower by subtraction of the dark current, but the value will depend on the details of the electronics of the sensing array coupled to the photodiode.[6]

The spectral current responsivity varies for the photosensors due to the transmittance of the transparent electrode and the absorbance of the BHJ. The average responsivity is 0.075 A/W (Ag, max. at 350/400 nm, 0.10 A/W), 0.069 A/W (Au, max. at 570 nm, 0.12 A/W), and 0.11 A/W (SLG, max. at 610 nm, 0.17 A/W) within the range of 250–650 nm. The UV transmittance of the top-illuminated photosensors is significantly improved in comparison to non-inverted photosensors (glass/ITO/PEDOT:PSS/P3HT:PCBM/Ca/Al) where the transmission decreases substantially at wavelengths shorter than 400 nm due to the ITO layer. An average current responsivity of 0.097 A/W was found for Ag at near UV (320–380 nm) with a slightly lower value for SLG of 0.083 A/W. The responsivity of photosensors with SLG at wavelengths below 300 nm was higher than that of devices with metal electrodes making it an attractive transparent electrode for UV photosensors.

Overall, the detectivity of the photodiodes with Ag electrodes was found to be the best of the three types of devices. Their performance was determined based on J_{dark} at low reverse bias ($V = -0.1$ V). Low applied voltages are favorable due to low device energy consumption and minimization of the dark current. The device-to-device variation of J_{dark} was examined and the maximum values were found to be 218 nA cm^{-2} (Au), 196 nA cm^{-2} (Ag), and 287 nA cm^{-2} (SLG) at $V = -0.1$ V. The lowest values of J_{dark} were 1.9 nAcm^{-2} for Au and Ag electrodes and 6.2 nA cm^{-2} using SLG. The variation in J_{dark} is attributed to doping of the active P3HT: PCBM layer by the contact metals and MoO_x and also shunts due to imperfections in processing. The calculated average detectivities using the optimal values (low

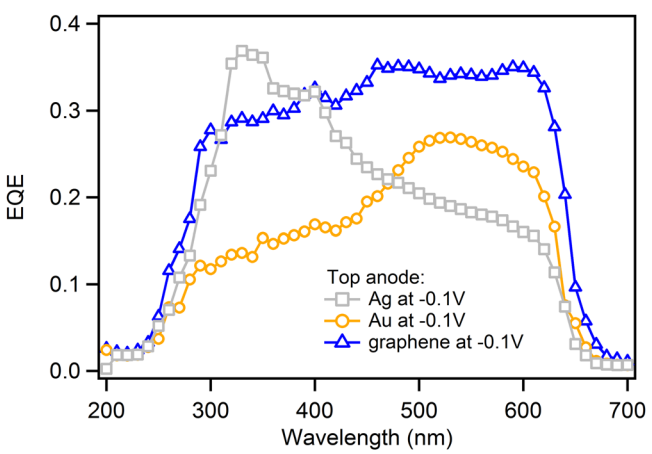

FIG. 3. External quantum efficiency versus wavelength for top-illuminated, inverted devices using Au, Ag, and SLG as top anodes at illumination intensity within the linear response regime.

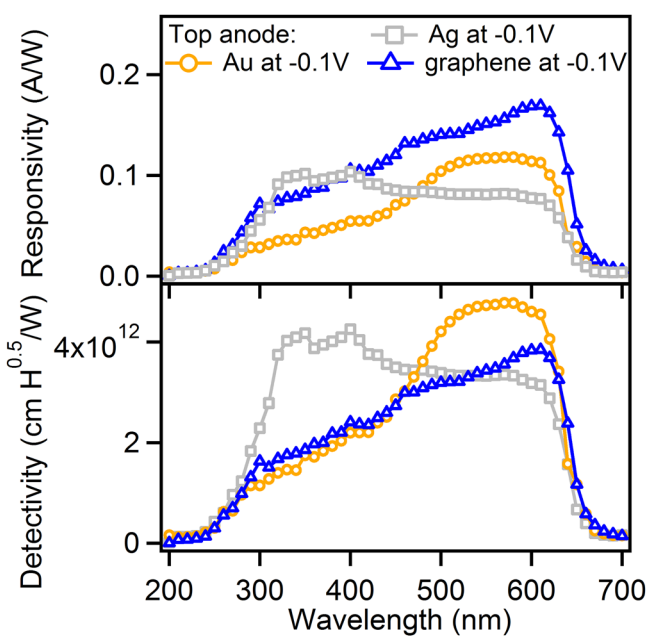

FIG. 4. Responsivity (a) and detectivity (b) of top-illuminated, inverted P3HT:PCBM photosensors with Au, Ag, and SLG top electrodes versus wavelength.

J_{dark}) are 3.1×10^{12} Jones (Ag), 2.8×10^{12} Jones (Au), and 2.5×10^{12} Jones (SLG) within the wavelength range of 250–650 nm. The higher value of J_{dark} leads to lower detectivity for the SLG devices and was attributed to the partial device preparation in air and water. We expect that J_{dark} would be reduced by transferring the graphene layer in an inert environment and would lead to improved characteristics compared to the other electrodes based on the better responsivity.

In conclusion, we have demonstrated inverted, top-illuminated BHJ photosensors with (semi-)transparent anodes of thin layers of Ag, Au, or SLG, which are free of both ITO and PEDOT:PSS. High spectral responsivity of 0.17 A/W for devices with SLG electrodes and detectivities around 3×10^{12} Jones are obtained, even though the BHJ was exposed to both air and water. The top illumination paired with a constant and high optical response over a broad spectral range (particularly SLG) makes them a promising candidate for organic photosensors on flexible substrates. Organic photosensors with SLG are particularly useful for detection of light at wavelengths less than 300 nm and have comparable responsivity to SiC photodiodes[33] despite the relative simplicity of fabrication.

M.B., C.G.S., and M.L.C. were supported by the Defense Threat Reduction Agency under award HDTRA1-10-1-0110. W.L. and K.B. were supported by the National Science Foundation under Award No. CCF-0811880. Portions of this work were carried out using UCSB MRL Central Facilities supported by the MRSEC Program of the NSF under Award No. DMR 1121053; a member of the NSF-funded Materials Research Facilities Network (www.mrfn.org). The authors would also like to thank Alexander A. Mikhailovsky for his help regarding optoelectronic characterization and Hong Li for many useful discussions.

[1]D. Birtalan and W. Nunley, *Optoelectronics: Infrared-Visible-Ultraviolet Devices and Applications*, 2nd ed. (CRC, Boca Raton, 2009).
[2]X. Gong, M. Tong, Y. Xia, W. Cai, J. S. Moon, Y. Cao, G. Yu, C.-L. Shieh, B. Nilsson, and A. J. Heeger, Science **325**, 1665 (2009).
[3]S.-H. Wu, W. L. Li, B. Chu, Z. Sheng Su, F. Zhang, and C. S. Lee, Appl. Phys. Lett. **99**, 023305 (2011).
[4]R. W. Waynant and M. N. Ediger, *Electro-Optics Handbook*, 2nd ed. (McGraw-Hill, New York, 2000).
[5]F. C. Krebs, S. A. Gevorgyan, and J. Alstrup, J. Mater. Chem. **19**, 5442 (2009).
[6]L.-M. Chen, Z. Hong, G. Li, and Y. Yang, Adv. Mater. **21**, 1434 (2009).
[7]T. N. Ng, W. S. Wong, M. L. Chabinyc, and R. A. Street, Appl. Phys. Lett. **92**, 213303 (2008).
[8]M. Wu, K. Pangal, J. C. Sturm, and S. Wagner, Appl. Phys. Lett. **75**, 2244 (1999).
[9]X. Tong, B. E. Lassiter, and S. R. Forrest, Org. Electron. **11**, 705 (2010).
[10]D. Baierl, B. Fabel, P. Gabos, L. Pancheri, P. Lugli, and G. Scarpa, Org. Electron. **11**, 1199 (2010).
[11]J.-Y. Lee, S. T. Connor, Y. Cui, and P. Peumans, Nano Lett. **10**, 1276 (2010).
[12]D. Baierl, B. Fabel, P. Lugli, and G. Scarpa, Org. Electron. **12**, 1669 (2011).
[13]X. Li, W. Cai, J. An, S. Kim, J. Nah, D. Yang, R. Piner, A. Velamakanni, I. Jung, E. Tutuc, S. K. Banerjee, L. Colombo, and R. S. Ruoff, Science **324**, 1312 (2009).
[14]S. Bae, H. Kim, Y. Lee, X. Xu, J.-S. Park, Y. Zheng, J. Balakrishnan, T. Lei, H. R. Kim, Y. I. Song, Y.-J. Kim, K. S. Kim, B. Özyilmaz, J.-H. Ahn, B. H. Hong, and S. Iijima, Nat. Nanotechnol. **5**, 574 (2010).
[15]Y. Hernandez, V. Nicolosi, M. Lotya, F. M. Blighe, Z. Sun, S. De, I. T. McGovern, B. Holland, M. Byrne, Y. K. Gun'Ko, J. J. Boland, P. Niraj, G. Duesberg, S. Krishnamurthy, R. Goodhue, J. Hutchison, V. Scardaci, A. C. Ferrari, and J. N. Coleman, Nat. Nanotechnol. **3**, 563 (2008).
[16]U. Stöberl, U. Wurstbauer, W. Wegscheider, D. Weiss, and J. Eroms, Appl. Phys. Lett. **93**, 051906 (2008).
[17]V. C. Tung, L.-M. Chen, M. J. Allen, J. K. Wassei, K. Nelson, R. B. Kaner, and Y. Yang, Nano Lett. **9**, 1949 (2009).
[18]J. S. Bunch, S. S. Verbridge, J. S. Alden, A. M. van der Zande, J. M. Parpia, H. G. Craighead, and P. L. McEuen, Nano Lett. **8**, 2458 (2008).
[19]J. Wu, H. A. Becerril, Z. Bao, Z. Liu, Y. Chen, and P. Peumans, Appl. Phys. Lett. **92**, 263302 (2008).
[20]Y. Wang, X. Chen, Y. Zhong, F. Zhu, and K. P. Loh, Appl. Phys. Lett. **95**, 063302 (2009).
[21]L. G. D Arco, Y. Zhang, C. W. Schlenker, K. Ryu, M. E. Thompson, and C. Zhou, ACS Nano **4**, 2865 (2010).
[22]G. Jo, S.-I. Na, S.-H. Oh, S. Lee, T.-S. Kim, G. Wang, M. Choe, W. Park, J. Yoon, D.-Y. Kim, Y. H. Kahng, and T. Lee, Appl. Phys. Lett. **97**, 213301 (2010).
[23]G. Greczynski, T. Kugler, and W. Salaneck, Thin Solid Films **354**, 129 (1999).
[24]K. W. Wong, H. L. Yip, Y. Luo, K. Y. Wong, W. M. Lau, K. H. Low, H. F. Chow, Z. Q. Gao, W. L. Yeung, and C. C. Chang, Appl. Phys. Lett. **80**, 2788 (2002).
[25]G. Li, V. Shrotriya, J. Huang, Y. Yao, T. Moriarty, K. Emery, and Y. Yang, Nature Mater. **4**, 864 (2005).
[26]W. Liu, H. Li, C. Xu, Y. Khatami, and K. Banerjee, Carbon **49**, 4122 (2011).
[27]M. Krögera, S. Hamwib, J. Meyerb, T. Riedlb, W. Kowalskyb, and A. Kahn, Org. Electron. **10**, 932 (2009).
[28]X. Wang, L. Zhi, and K. Müllen, Nano Lett. **8**, 323 (2008).
[29]M. Cox, A. Gorodetsky, B. Kim, K. S. Kim, Z. Jia, P. Kim, C. Nuckolls, and I. Kymissis, Appl. Phys. Lett. **98**, 123303 (2011).
[30]R. C. I. MacKenzie, T. Kirchartz, G. F. A. Dibb, and J. Nelson, J. Phys. Chem. C **115**, 9806 (2011).
[31]M. Razeghi and A. Rogalski, J. Appl. Phys. **79**, 7433 (1996).
[32]G. Yu, J. Wang, J. McElvain, and A. J. Heeger, Adv. Mater. **10**, 1431 (1998).
[33]D. M. Brown, E. T. Downey, M. Ghezzo, J. W. Kretchmer, R. J. Saia, Y. S. Liu, J. A. Edmond, G. Gati, J. M. Pimbley, and W. E. Schneider, IEEE Trans. Electron Devices **40**, 325 (1993).
[34]See supplementary material at http://dx.doi.org/10.1063/1.4733299 for UV-Vis transmittance spectra of the electrodes and current-voltage characteristics of the devices under AM 1.5 simulated solar illumination.